New Heterocyclic Organo-Chalcogenide Compounds: Synthesis, Physicochemical Characterization, and Evaluation of Anticancer Activity against Breast Cancer Cells

Hayat Hamza Abbas[1*], Majeed Yacoob Al-Luaibi[1], and Mohammed Jassem Al-Assadi[2]

[1]*Department of Chemistry, College of Science, University of Basrah, Basrah, 61004, Iraq*

[2]*Department of Laboratory Techniques, Faculty of Health and Medical Techniques, University of Almaaqal, Basrah, Iraq*

* ***Corresponding author:***

email: hayat.hamza@uobasrah.edu.iq

Received: June 20, 2022
Accepted: December 23, 2022

DOI: 10.22146/ijc.75582

Abstract: *This work aimed to synthesize, characterize and evaluate the thermal stability of new sulfur and selenium organochalcogenide derivatives and to test the cytotoxic activity against breast adenocarcinoma cell line (MCF-7) through conducting MTT assay and AO/EB dual staining-technique. Two series of ten organo-chalcogen compounds: 4-(substituted)phenylthiomorpholine-3,5-dione and 4-(substituted)phenylselenomorpholine-3,5-dione were prepared by the reaction of $Na_2S{\cdot}3H_2O$ and NaHSe with* N*-(substituted)phenyl-2-chloro-*N*-(2-chloroacetyl)acetamide, respectively, under nitrogen atmosphere to give the corresponding cyclic chalcogenide ligands. All new compounds were characterized by melting point, FTIR, elemental analysis, UV-Visible, ^{1}H-NMR and ^{13}C-NMR. Meanwhile, TG/DTA analysis of some of these ligands was conducted to evaluate the thermal stability, kinetic, and characteristic thermodynamic parameters. Absorption spectroscopy was used to investigate these compounds with human DNA. The experimental results investigated a hypochromic effect via intercalation binding mode. The role of the prepared ligands in breast cell lines has been investigated by conducting MTT assay via spectroscopic techniques on HBL100 and MCF-7, normal and cancer breast cell lines, respectively. Cell death was seen after AO/EB dye staining method employing the fluorescence microscopy technique. The results revealed that these compounds possess cytotoxic activity on the MCF-7 and HBL-100 cell lines at a fixed concentration.*

Keywords: *chalcogenide; phenylacetamide; seleno-morpholine; heterocyclic chalcogenide; thio-morpholine*

■ INTRODUCTION

Materials containing organochalcogens or coordination compounds with chalcogen bond(s) have been extensively investigated due to their unique properties, such as electric and thermal conductivities, molecular self-assemblies, nanotube formation, ion exchange capacity, non-linear optics, photoelectro-chemical behavior, and drug delivery [1-2].

Sulfur (S) and selenium (Se) compounds present several applications in a great variety of fields. The anticancer activity of these compounds was considered the most important application due to the burden, costs, and mortality rates caused by cancer disease [3-4].

Se is a crucial trace element [5-6] that is naturally occurring with both nutritional and toxicological properties. Se is non-toxic to humans in low concentrations, but it plays a significant role in human's health in addition to regulating many critical functions involving cells; therefore, an adduct that releases selenium to the biological system at a steading rate act as an effective pharmaceutical agent [7-10]. This is mediated by incorporating it into selenoproteins. Apparently, the effectiveness of Se adducts as an anti-infective or antioxidant agent depends on the bioavailability of Se at the site of action [11]. The use of Se in medicinal chemistry is helpful to care for many kinds of illness due to compatibility with the biological

system either directly or indirectly [7] e.g., Se supplements are given to repay its deficiency, while selenium sulfide is used in shampoos for the treatment of dandruff [12-13]. Moreover, through extensive experimental evidence *in vitro*, animal, and prospective studies, it emerged that the supplementation of Se reduces the incidence of different cancer types [14].

Natural heterocyclic five-membered ring compounds thiazolin-4-carboxylic acid (a derivative of formyl-cysteine), thiazolidine-4-carboxylic acid (thioproline), 2-amino-2-thiazoline-4-carboxylic acid (ATCA), and 2-amino-3-methyl-5-sulfanylimidazol-4-yl propanoic acid (ovothiol A) [15]. All these compounds demonstrated to possess different and, in some cases convergent biological activities such as oxygen and nitrogen-free radical scavenging capacity, detoxification of cyanide, and antioxidant activity [16].

Morpholine and thiomorpholine are organic heterocyclic compounds which have several practical applications as they are the most favorable organic solvent due to their low cost and can be considered good bases [17]. A large number of heterocyclic bases, such as thiomorpholine and their derivatives, have been reported [18] due to their thermal stability and bioinorganic applications such as antimalarial and antioxidant.

Our interest in this area is focused on the investigation of the thermal stability of the newly chalcogen ligands and on preparing compounds that may have an ability of cell-growth inhibition or have a selective or directed action on cancerous cells and to study the compound-DNA interactions of these chalcogen ligands by various techniques.

■ EXPERIMENTAL SECTION

Materials

All chemicals and solvents used were of analytical grade supplied by Sigma-Aldrich, Fluka, Merck, BDH, and SCH companies and were used as such without further purifications. Sodium carbonate, chloroacetyl chloride, sodium borohydride, and MTT stain were obtained from Sigma-Aldrich company. Dichloromethane was obtained from Fluka, USA. Dimethyl sulfoxide, sodium chloride, sodium hydroxide, and potassium hydroxide were obtained from Merck company. Selenium powder and chloroform were obtained from BDH. Absolute ethanol, acetone, and ethyl acetate were obtained from SCH. Normal (HBL-100) and cancer cell lines (MCF-7) were obtained from the IRAQ Biotech Cell Bank Unit in Basra and maintained in RPMI-1640 supplemented with 10% Fetal bovine, 100 units/mL penicillin, and 100 µg/mL streptomycin. Cells were passaged using Trypsin-EDTA reseeded at 70% confluence twice to third a week and incubated at 37 °C and 5% CO_2; the CO_2 incubator was obtained from Cypress Diagnostics (Belgium).

Instrumentation

The melting points of all prepared compounds were determined by a Buchi 510 melting point apparatus. FTIR (Fourier transform Infrared) spectra were recorded using an FTIR-8400S Shimadzu Spectrophotometer in the range (4000–400) cm^{-1} in KBr disk. Elemental analysis (C, H, N, S) was performed by using the EuroFA-Vector-EA-3000 Elemental Analyzer Apparatus. ^{1}H and ^{13}C-NMR spectra were recorded on a Bruker DRX 500 MHz and 125 MHz, respectively, using CD_3OD and DMSO-d_6 as internal standards (Central Laboratory, University of Tehran, Iran). UV-Vis spectra for ligands were measured on a Shimadzu 1800 UV-Vis spectrophotometer. The thermal analysis was carried out by NETZSCH STA449 F3 Jupiterg-Thermal analyzer.

Procedure

***General procedure for the synthesis of compound (4)* 2-Chloro-(substituted)phenyl acetamide.** A mixture of aryl amine compounds (4 mmol) and sodium carbonate (4.24 g; 4 mmol) in 70 mL of acetone was stirred for 30 min. Then, chloroacetyl chloride (6.5 mL; 8 mmol) was added dropwise. The reaction was stirred at room temperature for 2 h, filtered, and then the excess solvent was removed under a vacuum. To the filtrate, 30 mL of distilled water was added, and then the resulting solid was filtered, dried, and crystallized from ethanol/water (ratio 80:20) mixture [18-19] (see Scheme 1).

***N*-phenyl-2-chloro-*N*-(2-chloroacetyl) acetamide as compound (4a).** Follow the general procedure of 2-chloro-(substituted)phenyl acetamide(4) using aniline(1)

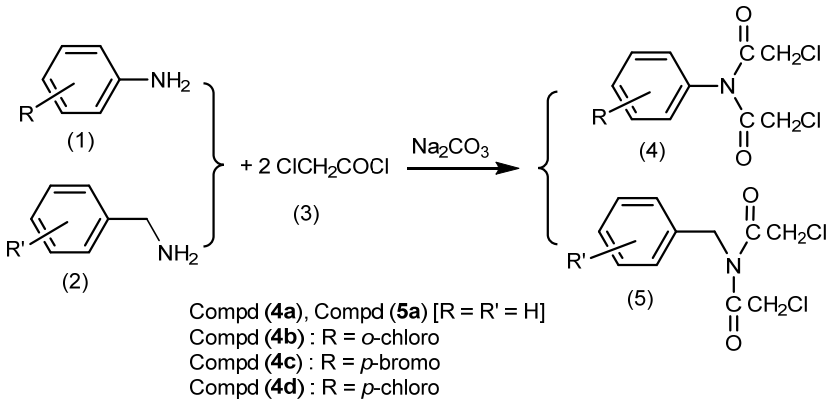

Scheme 1. Synthesis of *N*-aryl-2-chloro-*N*-(2-chloroacetyl)acetamide and their derivatives

(3.72 g; 4 mmol), sodium carbonate (4.24 g; 4 mmol) in 70 mL of acetone and chloroacetyl chloride (6.5 mL; 8 mmol). The silvery precipitate was obtained in 80% yield, m.p. 127–129 °C, IR νcm^{-1} (KBr): 1674 (C=O amide), 559 (C-Cl).

***N*-*o*-chlorophenyl-2-chloro-*N*-(2-chloroacetyl) acetamide as compound (4b).** Follow the general procedure of 2-chloro-(substituted)phenyl acetamide (4) using *o*-chloroaniline (5.14 g; 4 mmol), sodium carbonate (4.24 g; 4 mmol) in 70 mL .of acetone and chloroacetyl chloride (6.5 mL; 8 mmol). The white precipitate was obtained in 78% yield, m.p. 71–73 °C, IR νcm^{-1} (KBr): 1674 (C=O amide), 570 (C-Cl).

***N*-*p*-bromophenyl-2-chloro-*N*-(2-chloroacetyl) acetamide as compound (4c).** Follow the general procedure of 2-chloro-(substituted)phenyl acetamide (4) using *p*-bromoaniline (6.88 g; 4 mmol), sodium carbonate (4.24 g; 4 mmol) in 70 mL of acetone and chloroacetyl chloride (6.5 mL; 8 mmol). A chalky white precipitate was obtained in 75% yield, m.p. 191–193 °C, IR νcm^{-1} (KBr): 1670 (C=O amide), 567 (C-Cl).

***N*-*p*-chlorophenyl-2-chloro-*N*-(2-chloroacetyl) acetamide as compound (4d).** Follow the general procedure of 2-chloro-(substituted)phenyl acetamide (4) using *p*-chloroaniline (5.14 g; 4 mmol), sodium carbonate (4.24 g; 4 mmol) in 70 mL of acetone and chloroacetyl chloride (6.5 mL; 8 mmol). The white cotton precipitate was obtained in 82% yield, m.p. 177–179 °C, IR νcm^{-1} (KBr): 1670 (C=O amide), 567 (C-Cl).

***N*-benzyl-2-chloro-*N*-(2-chloroacetyl) acetamide as compound (5a).** Follow the general procedure of 2-chloro-(substituted)phenyl acetamide (4) using benzylamine (2) (3.55 g; 3.3 mmol), sodium carbonate (4.24 g; 4 mmol) in 70 mL of acetone and chloroacetyl chloride (6.5 mL; 8 mmol). The white transparent precipitate was obtained in 85%, yield m.p. 99–102 °C, IR νcm^{-1} (KBr): 1651 (C=O amide), 590 (C-Cl).

***General procedure for the synthesis of compound (6)* 4-(Substituted)phenylthiomorpholine-3,5-dione.** An aqueous solution of $Na_2S{\cdot}3H_2O$ (0.32 g; 2.00 mmol) was added to a solution of compound 4 (2.00 mmol) in 20 mL of ethanol under a nitrogen atmosphere. After about 30 min, a pale-yellow solution formed and filtered, then 50 mL of distilled H_2O was added, and the resulting solution was extracted with CH_2Cl_2 (30 mL) three times. The solvent was evaporated to a minimum amount; a pale-yellow precipitate was collected, then dried and recrystallized from ethanol (see Scheme 2).

4-Phenylthiomorpholine-3,5-dione as compound (6a). Follow the general procedure of 4-(substituted) phenylthiomorpholine-3,5-dione (6) using an aqueous solution of $Na_2S{\cdot}3H_2O$ (0.32 g; 2.00 mmol) and compound 4a (0.49 g; 2.00 mmol). White, yield: 83%, m.p. 172–174 °C, IR νcm^{-1} (KBr): 1651 (C=O amide), 752 (C-S), 1554 (C=C), 2914 (C-H_{al}), 3198 (C-H_{ar}), 3479 (C-OH), UV-Vis λ nm: 216 band I, 240 band II, 252 band III, Anal. Calculated for $C_{10}H_9NO_2S$: C, 57.95; H, 4.34; N, 6.76. Found: C, 56.79; H, 4.32; N, 6.74.

4-*o*-Chlorophenylthiomorpholine-3,5-dione as compound (6b). Follow the general procedure of 4-(substituted)phenylthiomorpholine-3,5-dione (6) using

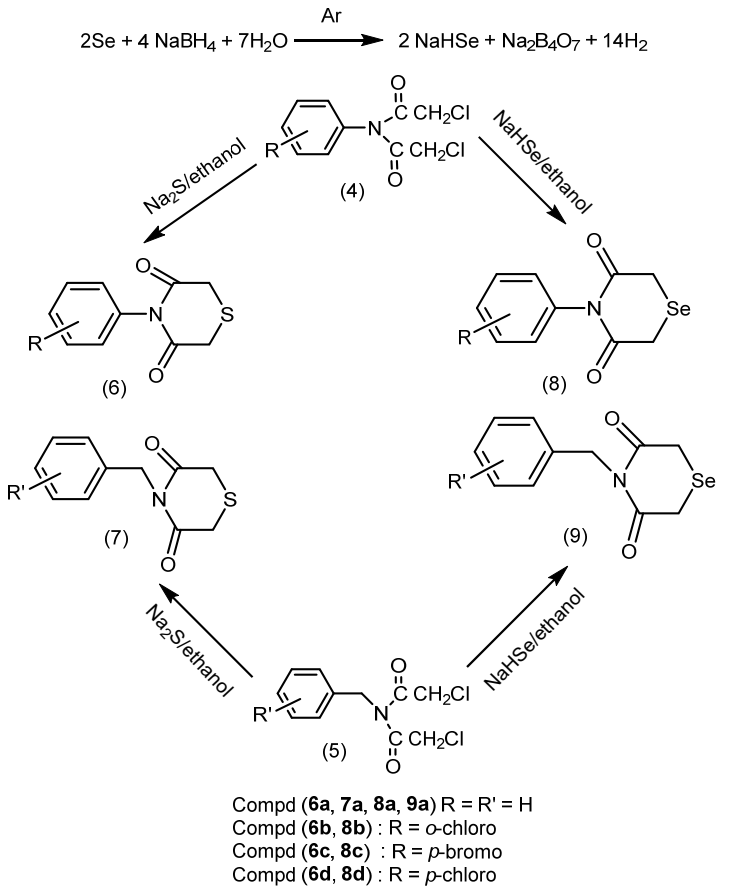

Scheme 2. Synthesis of chalcogenides (**6a**-**8d** and **9**) derivatives from *N*-aryl-2-chloro-*N*-(2-chloroacetyl) acetamide

an aqueous solution of $Na_2S{\cdot}3H_2O$ (0.32 g; 2.00 mmol) and compound 4b (0.56 g; 2.00 mmol). White, yield: 68%, m.p. 135–137 °C, IR νcm^{-1} (KBr): 1651 (C=O amide), 756 (C-S), 1531 (C=C), 2947 (C-H_{al}), 3036 (C-H_{ar}), 3452 (C-OH), ^{1}H-NMR spectra (ppm) DMSO-d_6 solvent: 2.55 ($1H_3$, s); 3.60 ($4H_1$, s); 7.19–7.15 ($1H_7$, t, Ar); 7.32–7.29 ($1H_8$, t, Ar); 7.49–7.47 ($1H_9$, d, Ar); 7.79–7.77 ($1H_6$, d, Ar), UV-Vis λ nm: 216 band I, 240 band II, 257 band III, Anal. Calculated for *o*-$ClC_{10}H_8NO_2S$: C, 49.48; H, 3.29; N, 5.77. Found: C, 49.50; H, 3.21; N, 5.78.

4-*p*-Bromophenylthiomorpholine-3,5-dione as compound (6c). Follow the general procedure of 4-(substituted)phenylthiomorpholine-3,5-dione (6) using an aqueous solution of $Na_2S{\cdot}3H_2O$ (0.32 g; 2.00 mmol) and compound 4c (0.65 g; 2.00 mmol). White, yield: 82%, m.p. 212–215 °C, IR νcm^{-1} (KBr): 1662 (C=O amide), 732 (C-S), 1543 (C=C), 2928 (C-H_{al}), 3037 (C-H_{ar}), 3502 (C-OH), ^{1}H and ^{13}C-NMR spectra (ppm) DMSO-d_6 solvent: 2.51 ($1H_3$, s); 3.37 ($4H_1$, s); 7.49–7.46 ($1H_6$ $1H_8$, d, Ar); 7.58–7.55 ($1H_5$ $1H_9$, d, Ar); 10.32 (OH, s) and 36.57 ($2C_1$); 155.41 (C_7); 121.57 (C_6, C_8); 132.00 (C_5, C_9); 138.83 (C_4); 168.18 (C_2, C_3), respectively, UV-Vis λ nm: 227 band I, 240 band II, 258 band III, Anal. Calculated for *p*-$BrC_{10}H_8NO_2S$: C, 41.81; H, 2.78; N, 4.87. Found: C, 41.77; H, 2.80; N, 4.85.

4-*p*-Chlorophenylthiomorpholine-3,5-dione as compound (6d). Follow the general procedure of 4-(substituted)phenylthiomorpholine-3,5-dione (6) using an aqueous solution of $Na_2S{\cdot}3H_2O$ (0.32 g; 2.00 mmol) and compound 4d (0.56 g; 2.00 mmol). White, yield: 80%, m.p. 183–185 °C, IR νcm^{-1} (KBr): 1662 (C=O amide), 740 (C-S), 1546 (C=C), 2935 (C-H_{al}), 3063 (C-H_{ar}), 3479 (C-OH), ^{1}H and ^{13}C-NMR spectra (ppm) DMSO-d_6 solvent: 2.44 ($1H_3$, s); 3.52 ($4H_1$, s); 7.38–7.35 ($1H_5$ $1H_9$, d, Ar); 7.64–7.61 ($1H_6$ $1H_8$, d, Ar); 10.36 (OH, s) and 38.71 ($2C_1$); 123.36 (C_6, C_8); 129.58 (C_4); 131.28 (C_5, C_9); 140.58 (C_7); 170.34 (C_2, C_3), respectively, UV-Vis λ nm: 227 band I, 240 band II, 258 band III, Anal. Calculated

for *p*-$BrC_{10}H_8NO_2S$: C, 49.48; H, 3.29; N, 5.77. Found: C, 49.51; H, 3.81; N, 5.76.

4-Benzylthiomorpholine-3,5-dione as compound (7a). Follow the general procedure of 4-(substituted) phenylthiomorpholine-3,5-dione (6) using an aqueous solution of $Na_2S{\cdot}3H_2O$ (0.32 g; 2.00 mmol) and compound 5a (0.52 g; 2.00 mmol). Pale-yellow, yield: 79%, m.p. 155–158 °C, IR νcm^{-1} (KBr): 1647 (C=O amide), 736 (C-S), 1535 (C=C), 2916 (C-H_{al}), 3032 (C-H_{ar}), 3425 (C-OH), UV-Vis λ nm: 227 band I, 237 band II, 251 band III, Anal. Calculated for $C_{11}H_{11}NO_2S$: C, 59.71; H, 5.01; N, 6.33. Found: C, 59.73; H, 5.11; N, 6.28.

General procedure for the synthesis of compound (8)

4-(Substituted)phenylselenomorpholine-3,5-dione. To a suspended solution of Se powder (0.14 g; 1.8 mmol) in 25 mL of H_2O has added a solution of $NaBH_4$ (0.118 g; 3.1 mmol) in 25 mL of H_2O under an argon atmosphere. A vigorous reaction occurs with the evolution of hydrogen gas. Se powder was consumed in less than 10 min, and a colorless solution of sodium hydrogen selenide NaHSe was formed [7]. To the resulting solution was added a solution of compound 4 (1.8 mmol) in 20 mL of ethanol under an argon atmosphere. After about 30 min, a colored precipitate was formed, collected by filtration and washed several times with ethanol, dried, and then Recrystallized from ethanol [20] (Scheme 2).

4-Phenylselenomorpholine-3,5-dione as compound (8a). Follow the general procedure of 4-(substituted) phenylselenomorpholine-3,5-dione (8) using a colorless solution of sodium hydrogen selenide NaHSe (prepared from the reduction of selenium with sodium borohydride) and a solution of compound 4a (0.48 g; 1.8 mmol) under argon atmosphere. Violet, yield: 83%, m.p. 172–174 °C, IR νcm^{-1} (KBr): 1647 (C=O amide), 497 (C-Se), 1554 (C=C), 2943 (C-H_{al}), 3144 (C-H_{ar}), 3290 (C-OH), UV-Vis λ nm: 216 band I, 240 band II, 252 band III, Anal. Calculated for $C_{10}H_9NO_2Se$: C, 47.25; H, 3.54; N, 5.51. Found: C, 47.22; H, 3.59; N, 5.49.

4-*o*-Chlorophenylselenomorpholine-3,5-dione as compound (8b). Follow the general procedure of 4-(substituted)phenylselenomorpholine-3,5-dione (8) using a colorless solution of sodium hydrogen selenide NaHSe (prepared from the reduction of selenium with sodium borohydride) and a solution of compound 4b (0.50 g; 1.8 mmol) under argon atmosphere. Pale gray, yield: 80%, m.p. 121–123 °C, IR νcm^{-1} (KBr): 1654 (C=O amide), 486 (C-Se), 1531 (C=C), 2952 (C-H_{al}), 3252 (C-H_{ar}), 3448 (C-OH), ^{1}H-NMR spectra (ppm) DMSO-d_6 solvent: 3.31 ($1H_3$, s); 3.63 ($4H_1$, s); 7.21–7.17 ($1H_7$, t, Ar); 7.34–7.31 ($1H_8$, t, Ar); 7.51–7.49 ($1H_9$, d, Ar); 7.81–7.79 ($1H_6$, d, Ar); 9.70 (OH, s), UV-Vis λ nm: 216 band I, 240 band II, 257 band III, Anal. Calculated for *o*-$ClC_{10}H_8NO_2Se$: C, 41.46; H, 2.76; N, 4.83. Found: C, 41.44; H, 2.75; N, 4.80.

4-*p*-Bromophenylselenomorpholine-3,5-dione as compound (8c). Follow the general procedure of 4-(substituted)phenylselenomorpholine-3,5-dione (8) using a colorless solution of sodium hydrogen selenide NaHSe (prepared from the reduction of selenium with sodium borohydride) and a solution of compound 4c (0.58 g; 1.8 mmol) under argon atmosphere. Pale gray, yield: 80%, m.p. 201–203 °C, IR νcm^{-1} (KBr): 1658 (C=O amide), 501 (C-Se), 1539 (C=C), 2939 (C-H_{al}), 3117 (C-H_{ar}), 3275 (C-OH), ^{1}H and ^{13}C-NMR spectra (ppm) DMSO-d_6 solvent: 2.51 ($1H_3$, s); 3.37 ($4H_1$, s); 7.49–7.46 ($1H_6$ $1H_8$, d, Ar); 7.58–7.55 ($1H_5$ $1H_9$, d, Ar); 10.32 (OH, s) and 3.33 ($1H_3$, s); 4.26 ($4H_1$, s); 7.52–7.47 ($1H_6$ $1H_8$, d, Ar); 7.57–7.53 ($1H_5$ $1H_9$, d, Ar); 10.27 (OH, s), respectively, UV-Vis λ nm: 240 band I, 258 band II, 271 band III, Anal. Calculated for *p*-$BrC_{10}H_8NO_2Se$: C, 35.94; H, 2.39; N, 4.19. Found: C, 35.89; H, 2.37; N, 4.21.

4-*p*-Chlorophenylselenomorpholine-3,5-dione as compound (8d). Follow the general procedure of 4-(substituted)phenylselenomorpholine-3,5-dione (8) using a colorless solution of sodium hydrogen selenide NaHSe (prepared from a reduction of selenium with sodium borohydride) and a solution of compound 4d (0.50 g; 1.8 mmol) under argon atmosphere. Pale pink, yield: 79%, m.p. 197–198 °C, IR νcm^{-1} (KBr): 1658 (C=O amide), 505 (C-Se), 1543 (C=C), 2939 (C-H_{al}), 3190 (C-H_{ar}), 3279 (C-OH), ^{1}H and ^{13}C-NMR spectra (ppm) DMSO-d_6 solvent: 3.55 ($1H_3$, s); 4.27 ($4H_1$, s); 7.39–7.35 ($1H_5$ $1H_9$, d, t, Ar); 7.62–7.59 ($1H_6$ $1H_8$, d, Ar); 10.28 (OH, s) and 29.57 ($2C_1$); 121.10 (C_7); 127.13 (C_6, C_8); 129.13 (C_5, C_9); 138.46 (C_4); 169.23 (C_2, C_3), respectively, UV-Vis λ nm: 216 band I, 240 band II, 258 band III,

Anal. Calculated for *p*-$ClC_{10}H_8NO_2Se$: C, 41.46; H, 2.76; N, 4.83. Found: C, 41.40; H, 2.66; N, 4.83.

4-Benzylselenomorpholine-3,5-dione as compound (9a). Follow the general procedure of 4-(substituted) phenylselenomorpholine-3,5-dione (8) using a colorless solution of sodium hydrogen selenide NaHSe (prepared from a reduction of selenium with sodium borohydride) and a solution of compound 5a (0.46 g; 1.8 mmol) under argon atmosphere. Pale violet, yield: 83%, m.p. 132–134 °C, IR νcm^{-1} (KBr): 1647 (C=O amide), 493 (C-Se), 1550 (C=C), 2920 (C-H_{al}), 3059 (C-H_{ar}), 3271 (C-OH), UV-Vis λ nm: 216 band I, 240 band II, 252 band III, Anal. Calculated for $C_{11}H_{11}NO_2Se$: C, 47.25; H, 3.54; N, 5.51. Found: C, 47.22; H, 3.59; N, 5.49.

Biological evaluation

Cytotoxicity is one of the most important indicators of biological evaluation test that use tissue cells (normal and cancer cell line); HBL-100 and MCF-7, respectively. The MTT assay is typically performed after the insoluble formazan produced is then solubilized by organic solvent such as DMSO (positive control), while serum-free media is considered as negative control.

Cytotoxicity measurement

To determine the cytotoxic effect of organo-chalcogen compounds; 4-(substituted)phenylthiomorpholine-3,5-dione (**6a**–**6d**, **7a**) and 4-(substituted)phenylseleno morpholine-3,5-dione (**8a**–**8d**, **9a**), the 3-(4,5-dimethylthiazole)-2,5-diphenyltetrazolium bromide (MTT) assay was used by reseeded [20] and then incubated at 37 °C and 5% CO_2. Cells were placed in 96-well micro assay culture plates (1×10^4) cells/well. After 24 h or a confluent monolayer was achieved, cells were treated with the tested compounds (I–X) (**6a**–**8d**, **9a**), which dissolved in DMSO at a concentration of 1000 µg/mL. Suspended cell with complete media 10% reseeded in 96-well plate 100 µL (1×10^4) cells/well, incubated at 37 °C and 100% humidity 5% CO_2. Untreated cells serve as a control group.

Cell viability was measured after 72 h of treatment by removing the medium, adding 28 µL of 2 mg/mL solution of MTT, and incubating the cells for 2 h at 37 °C. After removing the MTT solution, the crystals remaining in the wells were solubilized by the addition of 100 µL of DMSO and followed by 37 °C incubation for 15 min with shaking [21]. The optical density of each well was measured on a microplate reader at 620 nm (test wavelength). The assay was performed in triplicate to obtain mean values and the inhibition rate of cell growth. The percentage of cytotoxicity was calculated according to Eq. (1)

$$PR = \frac{B}{A \times 100} \quad (1)$$

where PR represents the proliferation rate, B represents the absorbance of compound-treated wells and A represents absorbance for a non-treated control group. Therefore, the inhibition rate (IR) was calculated using Eq. (2) [22].

$$IR = 100 - PR \quad (2)$$

Apoptosis studies with AO/EB staining method

Dual acridine orange/ethidium bromide (AO/EB) fluorescent staining, visualized under a fluorescent microscope**,** was employed to identify apoptosis-associated changes in cells during the process of apoptosis [23]. Dual fluorescent staining solution (1 µL) containing (5 mg/mL) acridine orange (AO) and (1 µL) containing (3 mg/mL) ethidium bromide (EB) was added to each 1 mL of phosphate buffer saline (PBS) and mixed well, then stored at room temperature and make fresh every few weeks before using. AO/EB stained MCF-7 cells. Cell death can occur in several modes when the cells are exposed to cytotoxic agents.

DNA binding experiments

The human-DNA interactive studies of compound **8a** were carried out in 5 mmol/L Tris-HCl and 5 mmol/L NaCl buffer (10 mM, pH = 7.2) which was prepared in deionized water. The 50 µM DNA stock in the buffer gave a ratio of UV absorbance at 260 and 280 nm of about > 1.86 indicating that the human DNA that was used for absorption titration was sufficiently free from protein [24].

The concentration of DNA per nucleotide was determined by using the molar absorption coefficient ε_{260} = 6600 M^{-1} cm^{-1}. The resulting DNA stock solution was kept at 4 °C and used within 24 h. A solution of 4-phenylselenomorpholine-3,5-dione (ligand **8a**) with

constant concentration 5×10^{-5} M, was prepared in 10% DMSO with 90% Tris-HCl buffer. Upon addition of varying concentrations of DNA stock solution (20–120 μM over 20 μM increments the resultant solutions) were incubated at 25 °C for 15 min before recording UV spectra [25]. The intrinsic binding constant (k_b) was determined by fitting the titration data into the following Eq. (3) [26]

$$\frac{[DNA]}{\varepsilon_a - \varepsilon_f} = \frac{[DNA]}{\varepsilon_b - \varepsilon_f} + \frac{1}{k_b(\varepsilon_b - \varepsilon_f)} \quad (3)$$

where ε_a, ε_f and ε_b are apparent, free, and bound ligand extinction coefficients, respectively. The ε_f was determined from a calibration curve of an isolated ligand following Beer's law. The ε_a matches the extinction coefficient of the particular absorption band at the specified DNA concentration (corresponding to A_{obs}/[complex], ε_b is equated to the extinction coefficient of a fully bound ligand to DNA. The plot of ([DNA])/($\varepsilon_a - \varepsilon_b$) versus [DNA], produces a slop 1/($\varepsilon_a - \varepsilon_f$) and a Y-intercept of 1/k_b($\varepsilon_b - \varepsilon_f$). The ratio of slope to the Y-intercept is expected to be the intrinsic binding constant (k_b).

■ RESULTS AND DISCUSSION

Thermogravimetric Study

The thermo-analytical methods (TG/DTA) were used in this work to evaluate the thermal stability, kinetic, and thermodynamic characteristic parameters. The thermal decomposition of some prepared ligands was done from ambient temperature to 800 °C under an argon atmosphere using α-Al_2O_3 as a reference. Kinetic parameters like frequency factor; Z; and activation energy, E_a of four chalcogen ligands were calculated from the Arrhenius plot of the rate of decomposition; Eq. (4-6) lnk v*ersus* I/T_s E_a was calculated from the slope and Z defined from the obtained intercept. The low value of Z indicates that the decomposition process was slow in nature [27]. The temperature of half weight loss ($T_{50\%}$), which represents the temperature at which the sample loses half of its total weight, has been appointed. The thermodynamic parameters (entropy ΔS^*, enthalpy ΔH^* and free energy ΔG^*) of the decomposing process were calculated by analyzing the TG curves mathematically using the Freeman-Carroll equation [28]. These calculations are dependent on the peak temperature T_s in order to get the highest rate of process Table 1. The negative value of ΔS^* indicates that the decomposition reactions proceed spontaneously and indicates that the activated ligands have more ordered structures than the reactants [29]. The thermal decomposition process of some of these ligands has one decomposition temperature (**7a**), while the others have two (**8d**, **6d**) or three (**6a**) decomposition temperatures (Fig. 2). The thermogram results show that the order of relative thermal stability of these ligands is **7a** > **8d** > **6d** > **6a** according to the decomposition temperature, while according to the crucial kinetic standards, the E_a values of these ligands take the order of **7a** < **6d** < **8d** < **6a**, which mostly differ from those defined by the thermal stability.

$$\Delta S^* = 2.303 \log\left(\frac{Zh}{k_b T_s}\right) R \quad (4)$$

$$\Delta H^* = E_a - RT_s \quad (5)$$

$$\Delta G^* = \Delta H^* - T\Delta S^* \quad (6)$$

In Vitro Cytotoxicity MTT Test

To assess the cytotoxic activity of the ten ligands (**6a**–**8d**), the cell viability was determined by the MTT test, a colorimetric assay determined by the mitochondrial-dependent reduction of soluble yellow tetrazolium salt to blue formazan crystals [30-31]. The data received from

Table 1. Thermal stability and thermodynamic parameters of prepared compounds

Compd	W_t	T_s [K]	Temp. of 50 wt.% loss (°C)	Rate of decomp.	Char. content 800 °C, (%)	Activation energy (E_a)	Temp. range (°C)	Z	ΔH^* (KJ/mol)	ΔS^* (J/mol k)	ΔG^* (KJ/mol)
6a	1.069	538.99	381.25	2.8	5.80	15.83	69–244	0.0012	11.35	−9.490	026.8
7a	2.163	578.33	246.00	3.4	15.0	14.07	67–172	0.0080	09.27	−275.7	168.7
6d	3.634	544.37	306.25	2.7	24.6	15.04	56–231	0.0003	10.51	−163.5	099.5
8d	1.568	550.91	321.50	3.4	8.20	15.63	125–250	0.0010	11.05	−324.6	289.5

this assay was analyzed by subtraction of the blank control absorbance value from all the other values. The DMSO-solvent control value is set to 100% viability, as no growth-inhibiting compound was added [32]. Fig. 3 shows the vitality of the cell line MCF-7 and normal breast cell line (HBL-100) when exposed to one concentration 1000 µg/mL for each one of the ten ligands (**6a**–**8d**) prepared. This concentration causes growth inhibition of normal and human MCF-7 breast cancer cells. The highest rate of vital percentage was 72.4% of *p*-chlorophenylthiomorpholine-3,5-dione (**6d**) ligand, while the lowest rate of vital percentage was 32% of 4-phenylselenomorpholine-3,5-dione (**8a**) ligand. While the normal cell line HBL-100, exposed to 4-phenylselenomorpholine-3,5-dione (**8a**) ligand and benzylselenomorpholine-3,5-dione (**9a**) ligand at the same concentration 1000 µg/mL for 72 h. The results showed that the vitality of the normal breast cell line was affected by these two ligands, **8a** and **9a**, and the rate of vital percentage was 30.9 and 39.3%, respectively. The percentage of cell viability was plotted against the concentration of compound added to the medium (Fig. 1).

AO/EB Staining and Programmed Cell Death

The AO/EB dye was employed to stain MCF-7 breast cancer cells that examine by fluorescence microscopic before and after treatment with compounds **8a** and **8c**. Thus, this assay was conducted to diagnose stages of programmed cell death. Cells that have undergone apoptosis are non-viable and emit red fluorescence upon binding of AO/EB to ssDNA or RNA, as the red blocks indicate the advanced stages of cell death. The viable cells colored green refer to the combined dye to dsDNA, while lumpy chromatin formed in yellow indicates the early stages of nucleus fragmentation and the appearance of cell death bodies [17].

Fig. 2 explores the microscopic fluorescence images of MCF-7 breast cancer cell line untreated (Fig. 2(a)) and treated AO/EB stained cells with compounds (**8a**) and (**8c**), Fig. 2(b) and 2(c), respectively. The untreated cells appear unaffected, showing a single integral monolayer of healthy and highly organized structure as they emit green fluorescence with AO/EB at magnification 10×. The MCF-7 cell line grill with AO/EB dye treated with compounds (**8a**), Fig. 2(b), and (**8c**), Fig. 2(c) appeared affected as they lost their normal characteristics. Thus, the appearance of the yellow-colored nucleus fragments indicates the early stages of programmed cell death showing large areas lacking cells at magnification 40× (Fig. 2(d) and 2(e)). The emergence of the large spaces devoid of cells in Fig. 2(e) reveals clearly that (**8c**) is more effective than compound (**8a**).

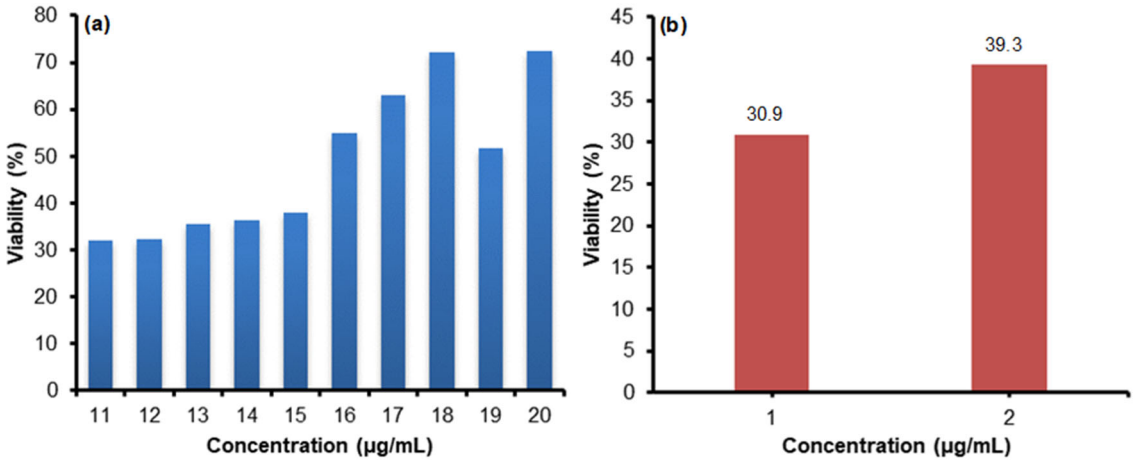

Fig 1. Percentage of cell viability in the cell line of **(a)** Breast cancer type (MCF-7) vs one concentration 1000 µg/mL for each one of the five (11–15) 4-(substutited)phenylselenomorpholine ligands (**8a**–**8d**), and of another five (16-20) 4-(substutited)phenylthiomorpholine ligands (**6a**–**6d**), (b) Normal breast cell line (HBL-100) vs one concentration 1000 µg/mL for each one of the two ligands (**1** and **2**) 4-phenylselenomorpholine ligand (**8a**) and 4-benzylselenomorpholine ligand (**9a**), respectively added to the medium

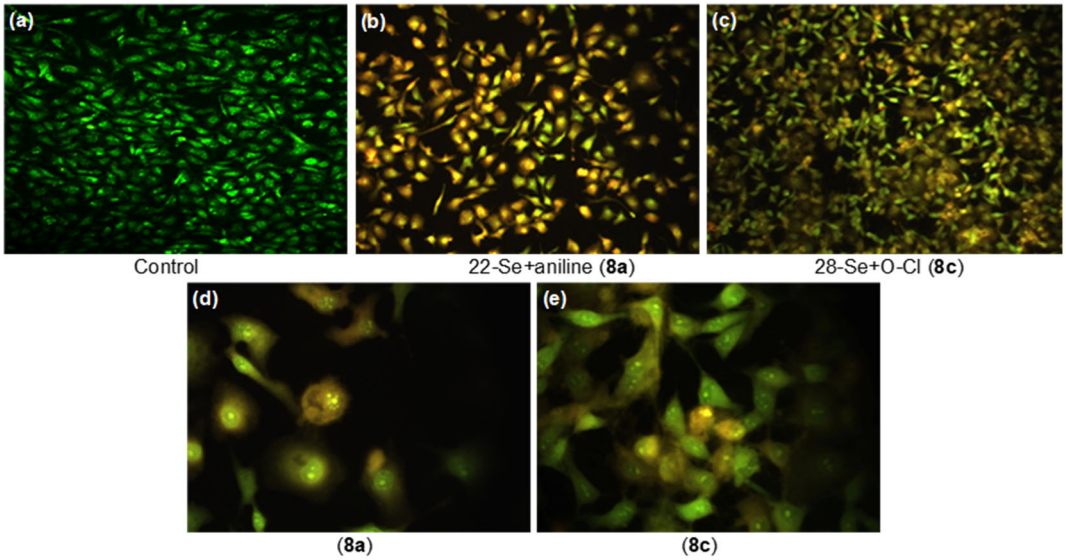

Fig 2. MCF-7 cell line dye AO/EB stain, (a) Untreated cells look unaffected, forming a monolayer strain green with AO/EB at magnification 10×, (b) Cells treated with compound (**8a**) appear affected as colored in yellow AO/EB at magnification 10×, (c) Cells treated with compound (**8c**); losing of normal characteristics refers to one of the early stages of cell death, AO/EB at magnification 10×. (d) and (e) images of (**8a**) and (**8c**) at magnification 40×

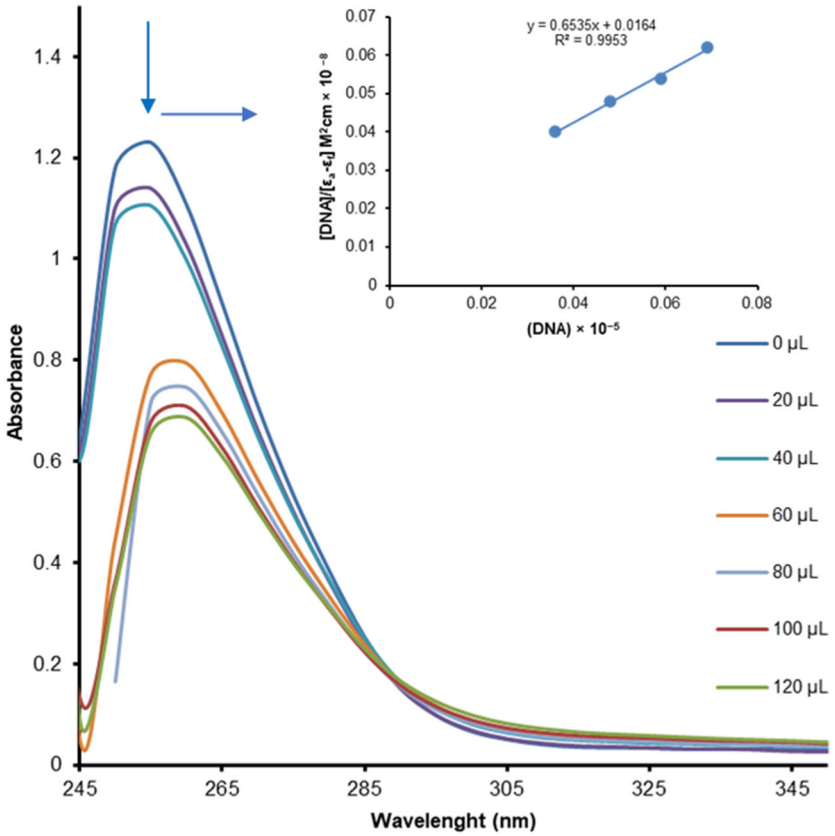

Fig 3. Overlay UV-Vis spectra of 4-phenylselenomorpholine, ligand (**8a**), in the absence and presence of increasing amounts of human-DNA. Arrow indicates that absorbance changes upon increasing DNA concentrations. Inset: Plot of $[DNA]/(\varepsilon_a - \varepsilon_f) \times 10^8$ vs $[DNA] \times 10^5$ and the linear fit for the titration

DNA-Binding

Absorption studies: the binding of prepared ligands to the helix has been characterized through the measurement of absorbance and the significant shift of maxima as a function of an added amount of DNA (20–120 μM) to a fixed ligands concentration (3.0×10^{-4} μM). For ligand **8a** (Fig. 3), the broadband at 260 nm was monitored as it has been noticed that an increase in the amount of DNA led to decreasing in molar absorptivity beside an 8–10 nm red shift i.e., a hypochromic shift indicating intercalative interaction of compound **8a** with DNA. The intrinsic binding constant was found to be $k_b = 3.60 \times 10^6$ M^{-1} suggesting moderate intercalative interaction, compared to classical intercalators ($k_b \sim 10^6$) function of added DNA. The isosbestic point at 290 nm confirms the bonding of ligands with DNA [33-34].

■ CONCLUSION

According to the decomposition temperature of the newly chalcogen ligands in the current study, the thermogram results show that the relative thermal stability of these ligands takes this order **7a** > **8d** > **6d** > **6a** while their activation energies E_a take another order **7a** < **6d** < **8d** < **6a** differs completely from that sequence. The results of absorption studies show that the absorption intensity decreased (hypochromic) evidently after the addition of DNA, which indicates that the interaction between DNA and ligand **8a** occurred. The intrinsic binding constant ($k_b = 3.42 \times 10^6$ M^{-1}) is roughly comparable to other intercalators' interactions. According to the toxicity by new ligands through the MTT-assay to both normal and cancerous lines, they have no selective or directed action on cancerous cells. Nevertheless, this method does not provide any information regarding the cell death mechanism, the phase in the cell cycle that is affected by the drug and its possible biological target. AO/EB assay and cell cycle analysis were conducted to diagnose stages of programmed cell death. It can be concluded that the low viability percentage of compounds **8a** and **8c** (Fig. 3), besides the cytofluorimetric inconclusive results, may indicate that these prepared compounds may have the ability of cell-growth inhibition. More studies need to be subjected to confirm this conclusion, such as the employment of variable concentrations of these compounds and increasing the time of exposure.

■ ACKNOWLEDGMENTS

The authors would like to acknowledge the University of Basrah, Faculty of Science, Department of Chemistry for supporting this work and Professor Ali Abd Allateef Abd Alhassan Al-Ali, Biological Department, College of Education for Basic Science, University of Basrah, for analyzing the cytotoxic effects.

■ AUTHOR CONTRIBUTIONS

Hayat Hamza Abbas who is a PhD student at the Chemistry Department at College of Science has done all the experiments with supervisors. All authors have read and approved the manuscript.

■ REFERENCES

[1] Garrett, G.E., Gibson, G.L., Straus, R.N., Seferos, D.S., and Taylor, M.S., 2015, Chalcogen bonding in solution: Interactions of benzotelluradiazoles with anionic and uncharged Lewis bases, *J. Am. Chem. Soc.*, 137 (12), 4126–4133.

[2] Alcolea, V., Garnica, P., Palop, J.A., Sanmartín, C., González-Peñas, E., Durán, A., and Lizarraga, E., 2017, Antitumoural sulphur and selenium heteroaryl compounds: Thermal characterization and stability evaluation, *Molecules*, 22 (8), 1314.

[3] Uivarosi, V., Badea, M., Aldea, V., Chirigiu, L., and Olar, R., 2013, Thermal and spectral studies of palladium(II) and platinum(IV) complexes with dithiocarbamate derivatives, *J. Therm. Anal. Calorim.*, 111 (2), 1177–1182.

[4] Zhou, G., Deng, X., Pan, C., Goh, E.T.L., Lakshminarayanan, R., and Srinivasan, R., 2020, SLAP reagents for the photocatalytic synthesis of C3/C5-substituted, *N*-unprotected selenomorpholines and 1,4-selenazepanes, *Chem. Commun.*, 56 (83), 12546–12549.

[5] Li, Q., Zhang, Y., Chen, Z., Pan, X., Zhang, Z., Zhu, J., and Zhu, X., 2020, Organoselenium chemistry-based polymer synthesis, *Org. Chem. Front.*, 7 (18), 2815–2841.

[6] Mamgain, R., Kostic, M., and Singh, F.V., 2023, Synthesis and antioxidant properties of organoselenium compounds, *Curr. Med. Chem.*, 29, 092986732966220801165849.

[7] Rother, M., and Quitzke, V., 2018, Selenoprotein synthesis and regulation in *Archaea*, *Biochim. Biophys. Acta, Gen. Subj.*, 1862 (11), 2451−2462.

[8] Solovyev, N.D., 2015, Importance of selenium and selenoprotein for brain function: From antioxidant protection to neuronal signalling, *J. Inorg. Biochem.*, 153, 1−12.

[9] Liu, T., Yang, T., Xu, Z., Tan, S., Pan, T., Wan, N., and Li, S., 2018, MicroRNA-193b-3p regulates hepatocyte apoptosis in selenium-deficient broilers by targeting MAML1, *J. Inorg. Biochem.*, 186, 235−245.

[10] Rangraz, Y., Nemati, F., and Elhampour, A., 2020, Selenium-doped graphitic carbon nitride decorated with Ag NPs as a practical and recyclable nanocatalyst for the hydrogenation of nitro compounds in aqueous media, *Appl. Surf. Sci.*, 507, 145−164.

[11] Du, P., Viswanathan, U.M., Xu, Z., Ebrahimnejad, H., Hanf, B., Burkholz, T., Schneider, M., Bernhardt, I., Kirsch, G., and Jacob, C., 2014, Synthesis of amphiphilic seleninic acid derivatives with considerable activity against cellular membranes and certain pathogenic microbes, *J. Hazard. Mater.*, 269, 74−82.

[12] Kamal, A., Nazari, M., Yaseen, M., lqbal, M.A., Ahamed, M.B.K., Majid, A.S.A., and Bhatti, H.N., 2019, Green synthesis of selenium-*N*-heterocyclic carbene compounds: Evaluation of antimicrobial and anticancer potential, *Bioorg. Chem.*, 90, 103042.

[13] Khalifa, M.E., Abdel-Hafez, S.H., Gobouri, A.A., and Kobeasy, M.I., 2015, Synthesis and biological activity of novel arylazothiazole disperse dyes containing selenium for dyeing polyester fibers, *Phosphorus, Sulfur Silicon Relat. Elem.*, 190 (4), 461−476.

[14] Cisnetti, F., and Gautier, A., 2013, Metal/N-heterocyclic carbene complexes: Opportunities for the development of anticancer metallodrugs, *Angew. Chem., Int. Ed.*, 52 (46), 11976−11978.

[15] Francioso, A., Conrado, A.B., Mosca, L., and Fontana, M., 2020, Chemistry and biochemistry of sulfur natural compounds: Key intermediates of metabolism and redox biology, *Oxid. Med. Cell. Longevity*, 2020, 8294158.

[16] Castellano, I., and Seebeck, F.P., 2018, On ovothiol biosynthesis and biological roles: From life in the ocean to therapeutic potential, *Nat. Prod. Rep.*, 35 (12), 1241−1250.

[17] Al-Harbi, S.A., Al-Saidi, H.M., Debbabi, K.F., Allehyani, E.S., Alqorashi, A.A., and Emara, A.A.A., 2020, Design and anti-tumor evaluation of new platinum(II) and copper(II) complexes of nitrogen compounds containing selenium moieties, *J. Saudi Chem. Soc.*, 24 (12), 982−995.

[18] Khalib, A.A.K., Al-Hazam, H.A.J., and Hassan, A.F., 2022, Inhibition of carbon steel corrosion by some new organic 2-hydroselenoacetamide derivatives in HCl medium, *Indones. J. Chem.*, 22 (5), 1269−1281.

[19] Hassan, A.F., Abdalwahed, A.T., Al-Luaibi, M.Y., and Aljadaan, S.A., 2021, Synthesis, characterization and thermal study of some new organochalcogenide compounds containing arylamide group, *Egypt. J. Chem.*, 64 (9), 5009−5015.

[20] Al-Ali, A.A.A., and Jawad, R.K., 2021, Cerium oxide nanoparticles CeO_2NP and retinoic acid trigger cytotoxicity and apoptosis pathway in human breast cell lines, *Ann. Rom. Soc. Cell Biol.*, 35 (4), 8448−8477.

[21] Al-Shammari, A.M., Al-Esmaeel, W.N., Al-Ali, A.A.A., Hassan, A.A., and Ahmed, A.A., 2019, Enhancement of oncolytic activity of Newcastle disease virus through combination with retinoic acid against digestive system malignancies, *Mol. Ther.*, 27 (4S1), 126−127.

[22] Freshney, R.I., 2015, *Culture of Animal Cells: A Manual of Basic Technique and Specialized Applications*, John Wiley & Sons, Hoboken, New Jersey.

[23] He, M., Du, F., Zhang, W.Y., Yi, Q.Y., Wang, Y.J., Yin, H., Bai, L., Gu, Y.Y., and Liu, Y.J., 2019,

Photoinduced anticancer effect evaluation of ruthenium(II) polypyridyl complexes toward human lung cancer A549 cells, *Polyhedron*, 165, 97−110.

[24] Abdel-Rahman, L.H., El-Khatib, R.M., Nassr, L.A.E., and Abu-Dief, A.M., 2017, DNA binding ability mode, spectroscopic studies, hydrophobicity, and *in vitro* antibacterial evaluation of some new Fe(II) complexes bearing ONO donors amino acid Schiff bases, *Arabian J. Chem.*, 10, S1835−S1846.

[25] Kaplanis, M., Stamatakis, G., Papakonstantinou, V.D., Paravatou-Petsotas, M., Demopoulos, C.A., and Mitsopoulou, C.A., 2014, Re(I) tricarbonyl complex of 1,10-phenanthroline-5,6-dione: DNA binding, cytotoxicity, anti-inflammatory and anti-coagulant effects towards platelet activating factor, *J. Inorg. Biochem.*, 135, 1−9.

[26] Bondi, R., Biver, T., Dalla Via, L., Guarra, F., Hyeraci, M., Sissi, C., Labella, L., Marchetti, F., and Samaritani, S., 2020, DNA interaction of a fluorescent, cytotoxic pyridinimino platinum(II) complex, *J. Inorg. Biochem.*, 202, 110874.

[27] Hsu, S.Y., Murphy, M.C., Smolensky, N.T., Vogels, C.M., Lebel, A.A., Masuda, J.D., Boudreau, L.H., Morin, P., and Westcott, S.A., 2023, Iminophosphine platinum(II) complexes containing long chain aniline derivatives: Synthesis, characterization, and anticancer properties, *Polyhedron*, 230, 116236.

[28] Gul, H., Shah, A.H.A., Gul, S., Arjomandi, J., and Bilal, S., 2018, Study on the thermal decomposition kinetics and calculation of activation energy of degradation of poly(*o*-toluidine) using thermogravimetric analysis, *Iran. J. Chem. Chem. Eng.*, 37 (1), 193−204.

[29] Song, M.Y., and Kwak, Y.J., 2022, Three methods for application of data from a volumetric method to the Kissinger equation to obtain activation energy, *Micromachines*, 13 (11), 1809.

[30] Patnaik, S., Panda, A.K., and Kumar, S., 2020, Thermal degradation of corn starch based biodegradable plastic plates and determination of kinetic parameters by isoconversional methods using thermogravimetric analyzer, *J. Energy Inst.*, 93 (4), 1449−1459.

[31] da Silva, M.M., de Camargo, M.S., Castelli, S., de Grandis, R.A., Castellano, E.E., Deflon, V.M., Cominetti, M.R., Desideri, A., and Batista, A.A., 2020, Ruthenium(II)-mercapto complexes with anticancer activity interact with topoisomerase IB, *J. Braz. Chem. Soc.*, 31 (3), 536−549.

[32] Ganot, N., Meker, S., Reytman, L., Tzubery, A., and Tshuva, E.Y., 2013, Anticancer metal complexes: Synthesis and cytotoxicity evaluation by the MTT assay, *J. Visualized Exp.*, 81, e50767.

[33] Swathy, S., Chandran, H., Reshma, G., Nakul, S., Kumar, M., Krishnan, M.A., Kulkarni, N.V., and Arakera, S.B., 2022, First row transition metal complexes of bis(3,5-dimethyl pyrazolyl)methane: Synthesis, molecular structure and antibacterial properties, *J. Mol. Struct.*, 1251, 132018.

[34] Tarai, S.K., Mandal, S., Bhaduri, R., Pan, A., Biswas, P., Bhattacharjee, A., and Moi, S.C., 2023, Bioactivity, molecular docking and anticancer behavior of pyrrolidine based Pt(II) complexes: Their kinetics, DNA and BSA binding study by spectroscopic methods, *Spectrochim. Acta, Part A*, 287, 122059.